ELSEVIER

Materials Science and Engineering A192/193 (1995) 474-482

MATERIALS SCIENCE & ENGINEERING A

Fatigue-crack growth and fracture resistance of a two-phase ($\gamma + \alpha_2$) TiAl alloy in duplex and lamellar microstructures

K.T. Venkateswara Rao[a], Y.W. Kim[b], C.L. Muhlstein[a], R.O. Ritchie[a]

[a]*Department of Materials Science and Mineral Engineering, University of California at Berkeley, Berkeley, CA 94720, USA*

[b]*Materials and Processing Division, UES, Inc., Dayton, OH 45324-1894, USA*

Abstract

The fatigue-crack propagation and fracture-toughness behavior of a two-phase ($\gamma + \alpha_2$) Ti-47.3Al-2.3Nb-1.5Cr-0.4V (in at.%) alloy in fine-equiaxed (duplex) and fully-lamellar microstructural conditions were examined at room temperature. It is observed that the lamellar microstructure displays superior fracture toughness and fatigue-crack growth resistance compared with the duplex microstructure, although the extent of improvement is significantly greater during quasi-static fracture. Crack extension under monotonic loading is characterized by resistance-curve behavior with plateau (steady-state) toughnesses of about 30 MPa $m^{1/2}$ in the fully-lamellar condition compared to a crack-initiation toughness of about 10 MPa $m^{1/2}$ for the duplex. Corresponding thresholds for cyclic fatigue-crack propagation are of the order of 10 and about 6.5 MPa $m^{1/2}$ in the lamellar and duplex structures, respectively. Such improved properties of the lamellar alloy are attributed principally to extrinsic shielding effects from tortuous crack paths, microcracking and formation of shear ligaments resulting from the microlaminated, composite-like features of the alloy.

Keywords: Fatigue; Cracking; Fracture; Titanium; Aluminium; Alloys

1. Introduction

Recent progress in alloying and microstructural control of γ-TiAl (ordered, face-centered tetragonal, $L1_0$ structure) based intermetallic alloys has led to the development of two-phase microstructures with marked improvements in ductility and fracture toughness at room temperature [1-12]. For example, Ti-(44-49)at.% Al alloys with 1-3at.% Nb, Cr, V or Mn and less than 0.5% Si, containing varying amounts of α_2-Ti_3Al (ordered hexagonal, DO_{19} structure) phase exhibit optimal ductility and toughness properties. Two classes of microstructure are prominent, namely lamellar structures consisting of alternating layers of ordered γ and α_2 platelets, obtained in the as cast condition or following thermal treatment in the α-phase field, and duplex microstructures consisting of equiaxed γ grains with small amounts of α_2 grains, obtained by heat treating in the ($\alpha + \gamma$) phase field.

Studies to date have shown that duplex microstructures display better tensile elongation values of up to 4%, yet low toughnesses below about 16 MPa $m^{1/2}$; in contrast, fully-lamellar microstructures with a large grain or colony size yield high fracture toughness values in excess of 20 MPa $m^{1/2}$, but low strength and ductility [9-12]. The improved fracture resistance of lamellar structures is attributed to crack deflection and branching at the α_2 phase, shear-ligament bridging by intact lath colonies in the crack wake, and mechanical slip/twinning of the γ-phase. Coarse-grained fully-lamellar structures also display markedly improved creep properties compared to duplex microstructures [9].

Despite advances made in the understanding of processing, microstructure and fracture toughness of two-phase ($\gamma + \alpha_2$) TiAl intermetallic alloys [1-12], there are only a few reports [13-15] on their fatigue-crack growth behavior and underlying microstructural damage mechanisms. Accordingly, the objective of the present study is to investigate systematically the fatigue-crack growth behavior in a two-phase ($\gamma + \alpha_2$) TiAl intermetallic alloy at room temperature, in both fine-grained duplex and coarse-grained fully-lamellar microstructures. The intent is to discern whether mechanisms responsible for toughening under monotonic loading conditions remain potent under cyclic loading. This aspect is of some significance because studies on ductile-particle-toughened intermetallic-

matrix composites [16,17] and grain-bridging ceramics [18,19] have shown that cyclic loads tend to reduce or diminish the efficacy of monotonic toughening mechanisms.

2. Materials and experimental methods

The Ti–47.3Al–2.3Nb–1.5Cr–0.4V alloy (G8) ingot was produced by skull-melting and casting techniques [10]. A billet was sectioned from the ingot, hot-isostatically pressed at 1150 °C under 275 MPa pressure for 3 h and then isothermally forged at 1150 °C to about 90% reduction. Two pieces were sectioned from the pancake shaped forging, about 10 mm thick and about 230 mm in diameter, and given two different thermal treatments in air as detailed below.

Duplex: annealing at 1300 °C for 2 h, controlled cool to 900 °C at 100 °C min^{-1}, aging at 900 °C for 5 h, air cool.

Lamellar: annealing at 1370 °C for 2 h, controlled cool to 900 °C at 30 °C min^{-1}, aging at 900 °C for 5 h, air cool.

The 1300 °C anneal and slow cooling results in a duplex microstructure consisting mainly of fine, equiaxed γ grains, about 15–40 μm in size, and about 5–10 vol.% of α_2 grains (Fig. 1(a)). Conversely, a fully-lamellar structure develops following annealing at 1370 °C and cooling (Fig. 1(b)), characterized by large grains (about 1–2 mm in size) with aligned layers of $\gamma + \alpha_2$ platelets and small amounts (less than 5 vol.%) of fine, equiaxed γ along the boundaries.

Reports on the tensile behavior of two-phase TiAl alloys at room temperature [10,11] indicate that duplex microstructures exhibit higher yield strength, ultimate strength and total elongation values than fully-lamellar microstructures, independent of strain rate and environment; properties of lamellar microstructures are additionally sensitive to colony size and lamellar spacing [20]. Effects of strain rate and environment are prominent at elevated temperatures, with tensile and fracture properties showing an inverse dependence on strain rate. Fully-lamellar structures are found to exhibit better strength retention at elevated temperatures; tensile properties for the two microstructures of an equivalent (G1) Ti–47Al–2.6Nb–2(Cr+V) alloy [10,11] are summarized in Table 1.

Fatigue-crack propagation behavior was examined at room temperature in a moist air environment (22 °C, 45% relative humidity) using 25 mm wide and 5 mm thick compact-tension C(T) specimens [21]. Samples were fabricated by electrodischarge machining with a wedge-shaped (semi-chevron) starter notch to facilitate

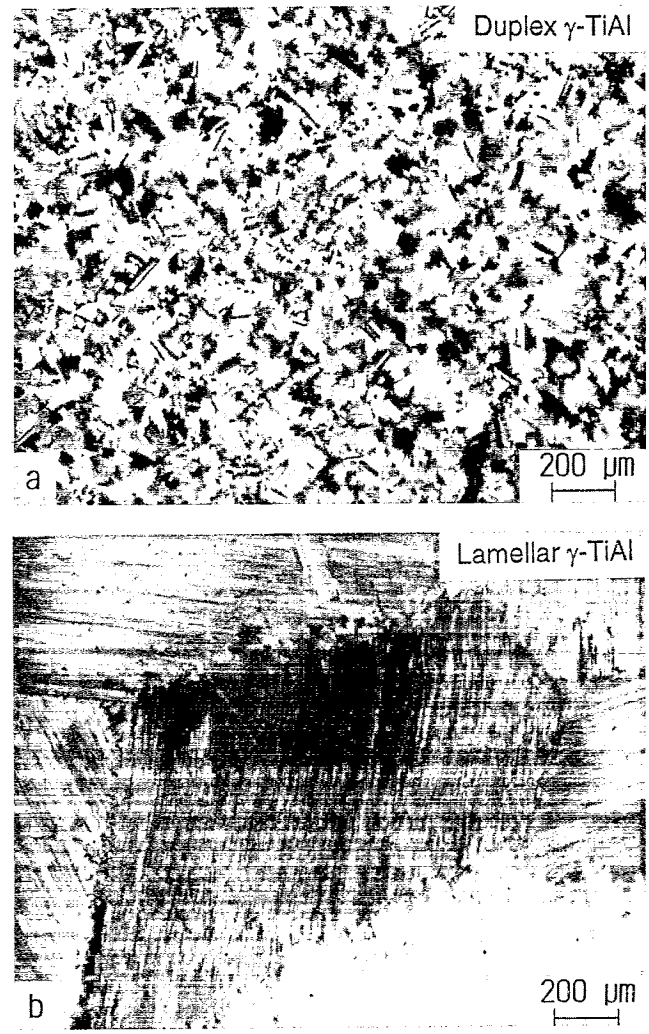

Fig. 1. Optical metallographs of the dual-phase ($\alpha_2+\gamma$) Ti–47.3Al–2.3Nb–1.5Cr–0.4V–1.9Nb alloy thermally treated to yield (a) fine-grained duplex and (b) coarse-grained fully-lamellar microstructures.

precracking under cyclic tension–tension loads. Tests were performed using electro-servo-hydraulic machines operating under automated stress-intensity K control at a load ratio R (ratio of the minimum to maximum stress intensity, K_{min}/K_{max}) of 0.1 and a frequency of 25 Hz (sine wave).

Crack lengths were continuously monitored to a resolution better than ± 5 μm from electrical resistivity changes in thin metallic foils bonded to the specimen surface; measurements were verified by in situ observations on the specimen surface, using a high-resolution optical telescope equipped with a video camera. Specifically, discontinuous cracking in the lamellar microstructure at high stress-intensity levels results in the formation of bridges in metal foils and complicates the reliability of crack length estimates based on bonded gages. Cyclic crack-growth results are presented in terms of the crack-growth rate per cycle

Table 1
Summary of mechanical properties for two-phase ($\gamma + \alpha_2$) Ti–47Al–2.6Nb–2(Cr + V) intermetallic alloys[a] [2,10,11]

Microstructure	Test condition	Yield strength σ_y (MPa)	Ultimate strength σ_0 (MPa)	Tensile elongation (%)	Fracture toughness[b] K_{Ic} (MPa $m^{1/2}$)
Duplex	25 °C–air	415	558	3.7	11.4
	600 °C–air	342	600	7.3	16.1
	790 °C–vacuum	168	296	13.0	—
Lamellar	25 °C–air	330	383	0.9	18–33
	25 °C–vacuum	330	375	0.8	16–25
	800 °C–air	300	396	9.0	35–75
	800 °C–vacuum	309	602	29.0	35–61

[a]Reported values are for the slowest strain rate in tension.
[b]Range indicates R-curve behavior; the initiation and plateau toughness values are listed.

da/dN as a function of the applied stress-intensity range ΔK ($K_{max} - K_{min}$). In addition, the extent of premature crack closure and crack bridging was assessed using back-face strain compliance methods [22].

Fracture toughness behavior was examined by loading the fatigue tested samples monotonically to failure; tests were performed in general accordance with ASTM Standard E399 [23] with loading and displacement rates ranging between 1.2–1.5 N s^{-1} and 4–5 μm s^{-1}, respectively. Crack length and crack–particle interactions were monitored using the high-resolution telescope/video camera system. Failures in the duplex microstructure were catastrophic with no stable crack growth prior to fracture. In the lamellar microstructure, crack initiation was followed by a load drop associated with the nucleation of a microcrack ahead of the main crack-tip. Following direct observation of crack nucleation or crack extension, loads were reduced (by about 15–20%) to stabilize further cracking; the new crack length was noted and loads were again increased to further extend the crack. Results are presented in terms of resistance curves, i.e. fracture resistance K_R as a function of crack extension Δa.

Crack-path profiles in the plane of loading were examined using optical and scanning electron microscopy (SEM) by taking metallographic sections parallel to the crack growth direction at specimen mid-thickness ($t/2$) location. Fracture surfaces were imaged using SEM.

It should be noted that in order to assure a representative evaluation of the mechanical properties of engineering materials for large-scale structures, laboratory test methods should reflect (i) plane-strain conditions (if appropriate), (ii) small-scale bridging, and (iii) a statistical sampling of the microstructure (i.e. polycrystalline constraint). These factors assume particular significance for coarse-grained microstructures such as the lamellar γ-TiAl alloy. First, to achieve plane-strain conditions stipulated by ASTM Standard E399 [23] for fracture toughness measurement in the lamellar microstructure, test specimens with thicknesses in excess of about 10 mm would be required. Secondly, the uncracked ligament size should exceed about 9 mm (roughly three times the bridging zone length of about 3 mm) to satisfy small-scale bridging requirements. Finally, in order to establish polycrystalline constraint during both fatigue and fracture, the crack front should sample at least 10–100 grains; for the lamellar γ-TiAl alloy, this necessitates testing of laboratory specimens with thicknesses between 20 and 200 mm.

Clearly, in the present study, all of the above size requirements have not been met for the lamellar microstructure due to limitations in processing of suitable material. Accordingly, fracture toughness results obtained will likely be dependent on sample geometry and size; however, small-scale bridging and plane-strain conditions are prevalent under cyclic fatigue loading due to the relatively small bridging zones at ΔK levels below 15 MPa $m^{1/2}$. It is important, though, that engineering mechanical property evaluation of lamellar γ-TiAl alloys must include the effect of larger sample size on fracture and fatigue properties if these alloys are to be seriously considered for structural application.

3. Results

3.1. Crack-growth behavior

Fatigue-crack propagation behavior at $R = 0.1$ under cyclic loading for the duplex and lamellar microstructures of the two-phase Ti–47.3Al–2.3Nb–1.5Cr–0.4V alloy is shown in Fig. 2; results for a single-phase γ-

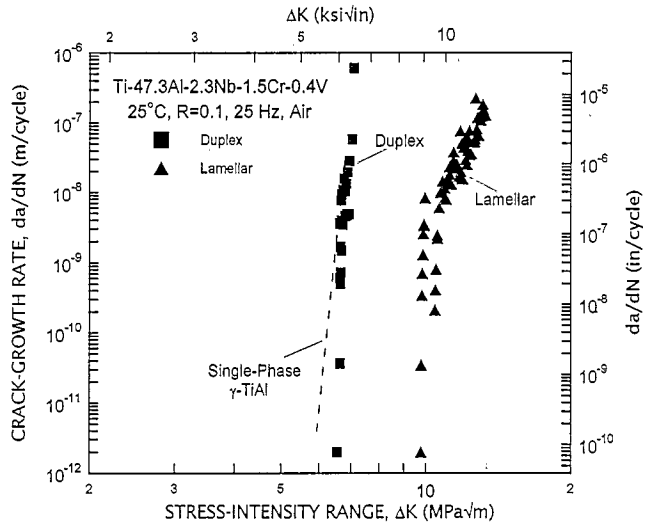

Fig. 2. Fatigue-crack growth behavior of the two-phase γ-TiAl alloy in the duplex and lamellar microstructures at room temperature in air (R = 0.1, 25 Hz); results in single-phase γ-TiAl [17] are also shown for comparison. Note the improved cyclic crack-growth resistance of the lamellar structure compared with the duplex.

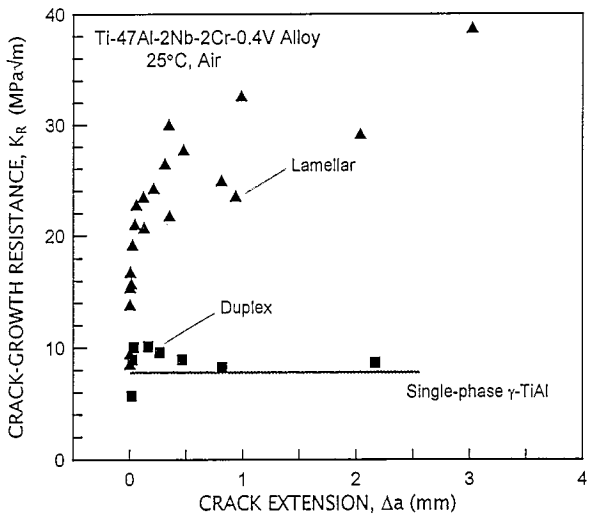

Fig. 3. Fracture-toughness behavior of the two phase TiAl alloy in the duplex and lamellar microstructures under monotonic loading at room temperature in air; behavior in single-phase γ-TiAl is also shown for comparison.

TiAl (Ti–50.5at.%Al) alloy [17] are also plotted for comparison. Corresponding fracture resistance of these microstructures under monotonic loading is illustrated in Fig. 3. From these data it is evident that the duplex microstructure yields only a marginal improvement in fatigue-crack growth and fracture resistance over single-phase γ-TiAl alloys. Moreover, the duplex alloy exhibits catastrophic brittle fracture under monotonic loading without significant stable crack extension prior to failure; a crack-initiation toughness of about 10 MPa $m^{1/2}$ was measured, which is slightly higher than the K_{Ic} value of about 8 MPa $m^{1/2}$ for pure γ-TiAl.

Under cyclic loading, subcritical crack growth in the duplex microstructure is seen at stress intensities of 6–7 MPa $m^{1/2}$, approximately 40% below those required for unstable fracture. Moreover, akin to most brittle ceramic and intermetallic materials [16–19], crack-growth rates are extremely sensitive to the applied ΔK level, spanning nearly six orders of magnitude for less than 1 MPa $m^{1/2}$ change in applied stress intensity. Expressed in terms of the empirical Paris power-law relationship:

$$da/dN = C\Delta K^m$$

the exponent is about 50, comparable with values measured for ceramics [18,19] and single-phase γ-TiAl [17]; exponents for ductile metals and alloys range from 2 to 4 [24,25]. With exponents so large, crack-growth rate data show no evidence of a sigmoidal relationship with stress-intensity range (i.e. with near-threshold (stage I), intermediate (stage II) and high-growth rate (stage III) regimes, as commonly seen in ductile metallic materials).

By contrast, a marked enhancement in fatigue-crack growth and fracture resistance is observed when the γ-TiAl alloy is thermomechanically treated to generate a fully-lamellar microstructure consisting of aligned $(\gamma + \alpha_2)$ microlaminate colonies or grains. The entire da/dN–ΔK curve is shifted to the right by nearly 4 MPa $m^{1/2}$. The measured fatigue-threshold stress-intensity range ΔK_{TH}, of about 10 MPa $m^{1/2}$, is over 70% higher than for the duplex and single-phase γ-TiAl alloys. Two distinct regions are apparent on the crack-growth curve for the lamellar alloy. For da/dN below about 10^{-9} m $cycle^{-1}$, growth rates are highly sensitive to the applied ΔK, similar to the near-threshold response in metals; above $da/dN \sim 10^{-9}$ m $cycle^{-1}$ (intermediate growth-rate region) the lamellar structure shows improved crack-growth resistance over the duplex microstructure, as evident from the milder dependence of growth rates on applied ΔK (power-law exponent, $m \sim 15$).

However, the extent of improvement in fatigue-crack growth resistance (assessed in terms of the ΔK level necessary to propagate the crack at a given growth rate) of the lamellar microstructure under cyclic loading is lower than the corresponding elevation in fracture toughness achieved under monotonic loading. As shown in Fig. 3 and reported elsewhere [8–12], the lamellar structure exhibits a crack-initiation toughness of about 20 MPa $m^{1/2}$ during quasi-static loading with the fracture resistance increasing with crack extension (R-curve behavior). After about 3 mm of crack growth the toughness reaches about 40 MPa $m^{1/2}$, which represents nearly a four-fold increase over single-phase and

duplex γ-TiAl toughnesses of about 8 and about 10 MPa $m^{1/2}$, respectively.

3.2. Crack/microstructure interactions

Corresponding crack–microstructure interactions in the two microstructures under monotonic and cyclic loading conditions are illustrated by SEM and optical micrographs in Figs. 4–8. Failures under monotonic loading in the duplex microstructure are characterized predominantly by transgranular cleavage of the γ grains (Fig. 4), consistent with the occurrence of unstable fracture during quasi-static loading. The features are similar under cyclic loading except for the characteristic parallel slip markings or features within grains (Fig. 5(c)), in addition to the static, transgranular cleavage mode of failure. Such clear differences in

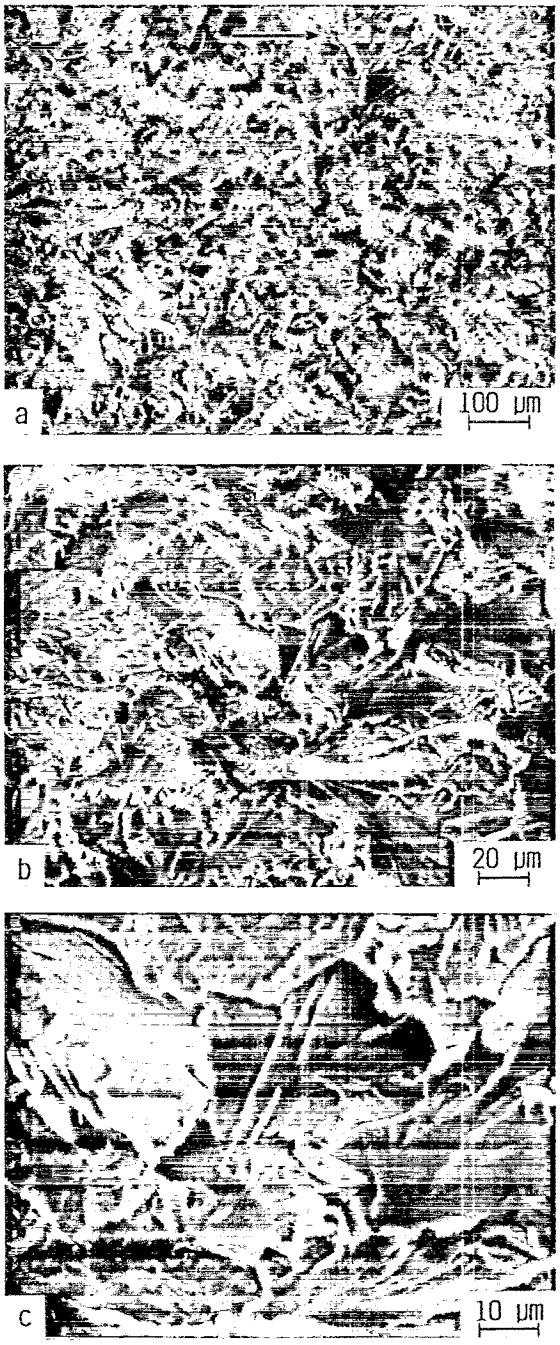

Fig. 4. Scanning electron micrographs of fracture surfaces in the duplex γ-TiAl alloy under monotonic loading at various magnifications ($K \sim 10$ MPa $m^{1/2}$, 25 °C, air). Horizontal arrow indicates the crack-growth direction.

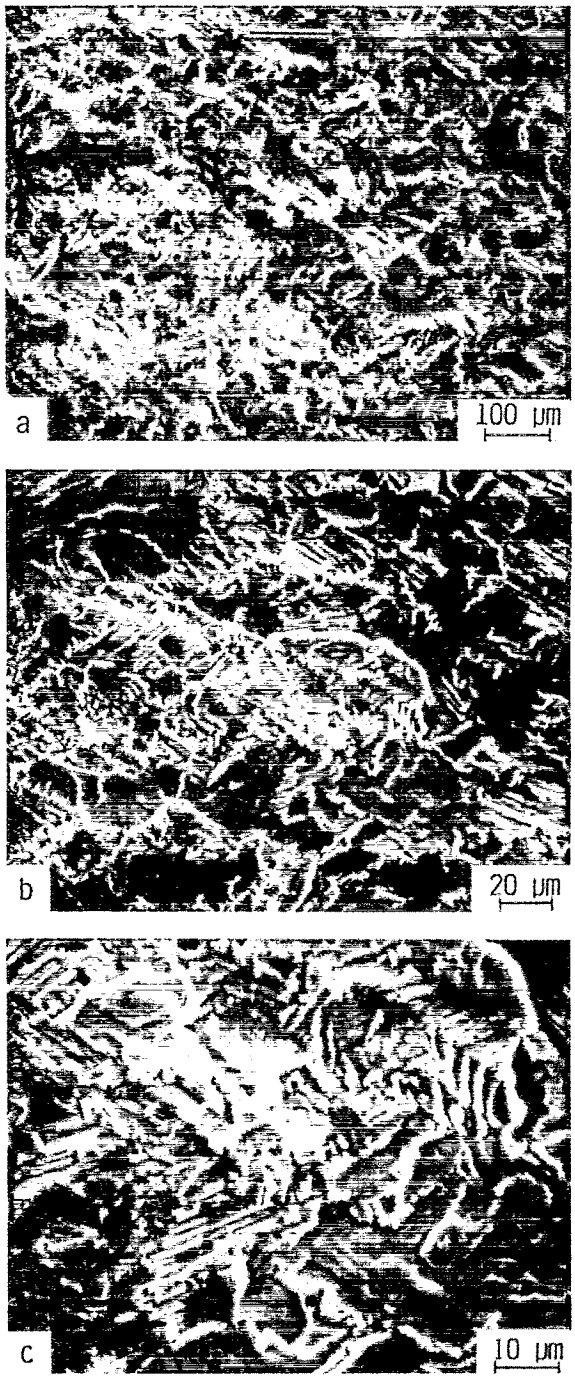

Fig. 5. Scanning electron micrographs of fracture surfaces in the duplex γ-TiAl alloy under cyclic loading at various magnifications ($\Delta K \sim 6.8$ MPa $m^{1/2}$, 25 °C, air). Horizontal arrow indicates the crack-growth direction.

monotonic vs. cyclic failure morphologies suggest that the deformation mechanism in the duplex microstructure during fatigue is different from that during quasi-static fracture. Fracture paths under monotonic and fatigue loading are linear (Fig. 6) and show evidence of microcracking in the γ grains ahead of the main crack tip.

Fractographic features in the lamellar alloy are more complex and tend to vary from grain to grain depending on their orientation to the principal stress–crack plane (Figs. 7, 8). On a macroscopic scale, monotonic and fatigue fracture surfaces are unusually rough, resembling plywood-type failures seen in wood-based materials due to the laminated structure within each grain (Figs. 7(a), 8(a); the surface roughness, however, is larger during monotonic fracture. On a finer scale, surfaces of individual γ and α_2 plies are rather flat and featureless, indicative of cleavage-like, translamellar separation during quasi-static fracture (Fig. 7(c)), with secondary interlamellar delamination cracking between the γ–α_2 or γ–γ platelet interfaces (Fig. 7(b)). In general, features noted during monotonic fracture

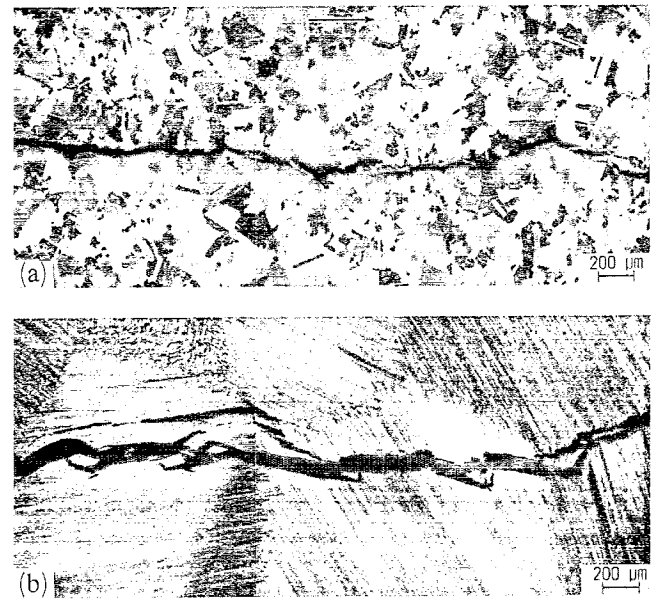

Fig. 6. Cyclic crack-growth morphologies in the $(\alpha_2+\gamma)$ Ti–47.3Al–2.3Nb–1.5Cr–0.4V–1.9Nb alloy processed in the (a) duplex and (b) lamellar microstructural conditions at 25 °C in air. Horizontal arrow indicates the direction of crack growth.

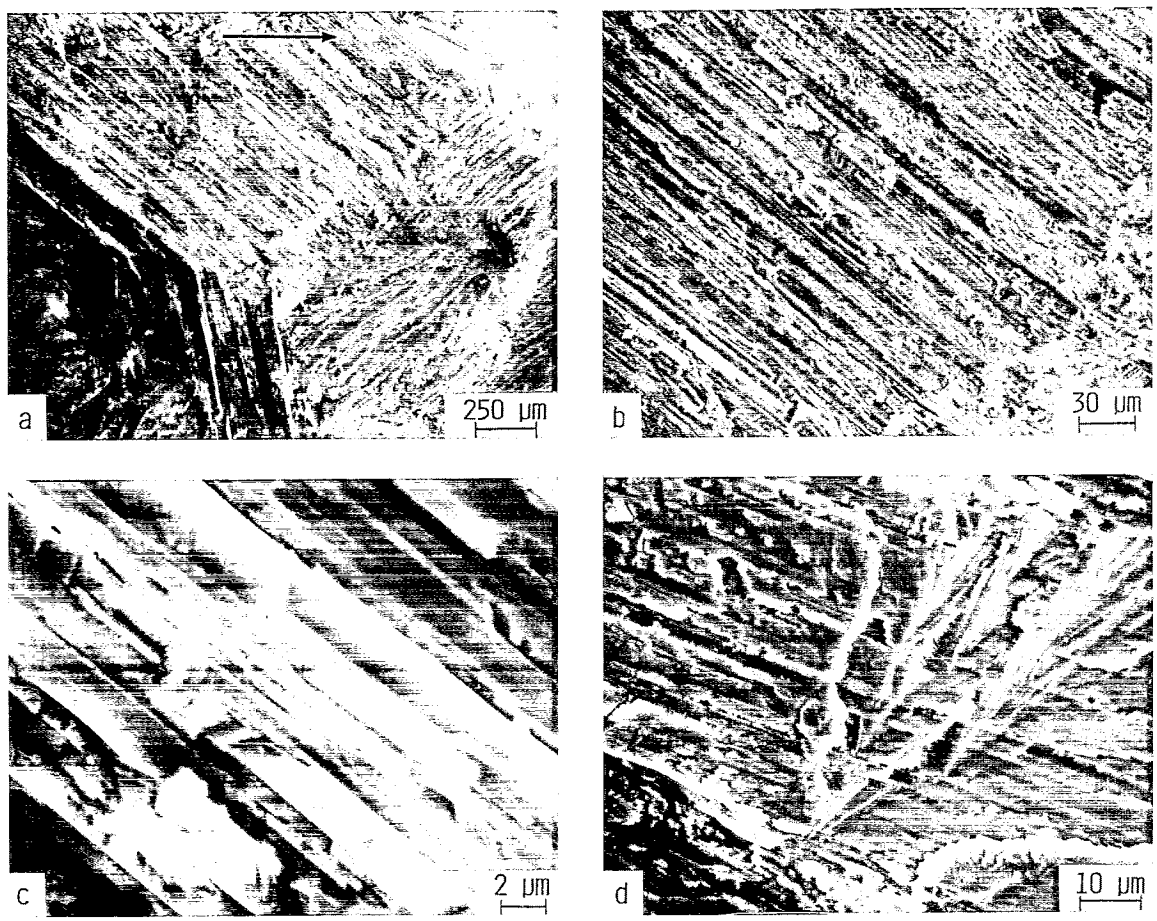

Fig. 7. Scanning electron micrographs of fracture surfaces in the lamellar γ-TiAl alloy under monotonic loading at various magnifications ($K \sim 22$ MPa $m^{1/2}$, 25 °C, air). Horizontal arrow indicates the crack-growth direction.

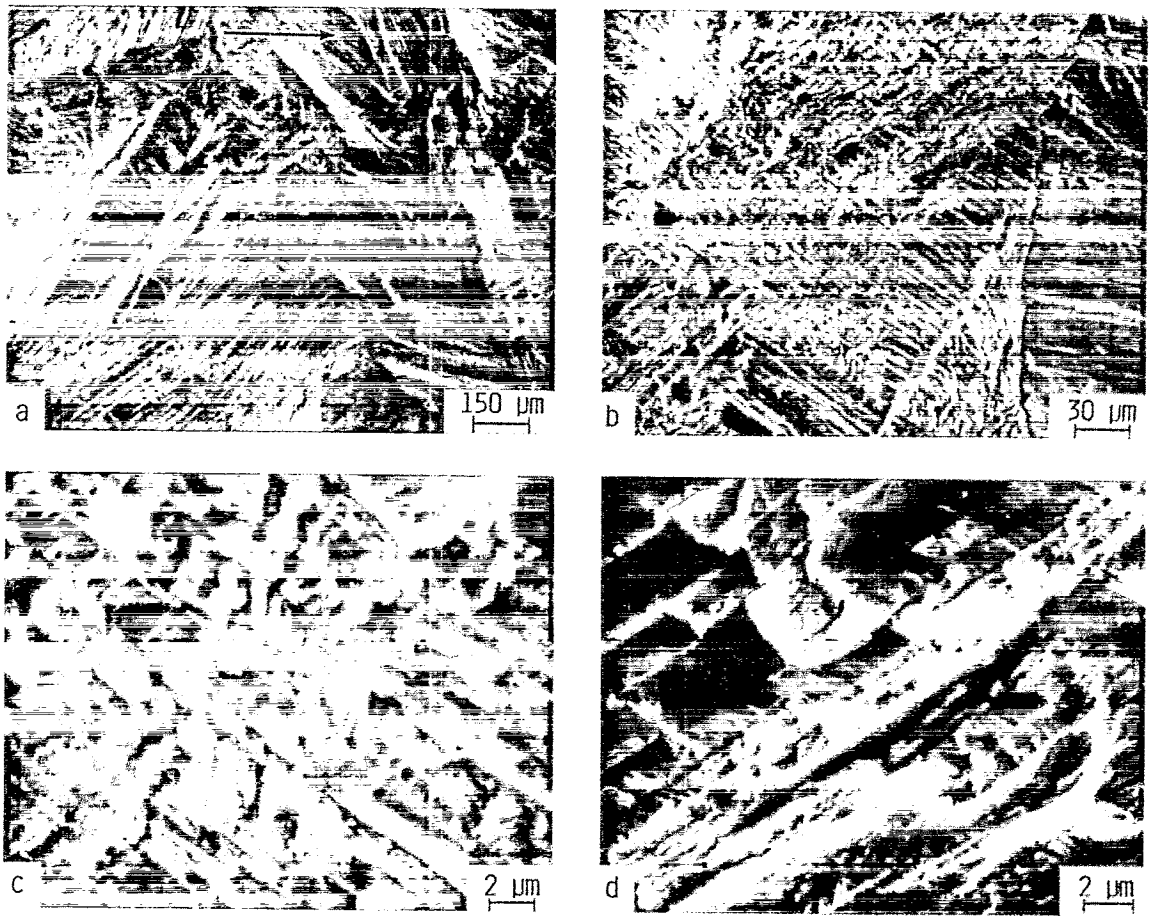

Fig. 8. Scanning electron micrographs of fracture surfaces in the lamellar γ-TiAl alloy under cyclic loading at various magnifications ($\Delta K \sim 12$ MPa $m^{1/2}$, 25 °C, air). Horizontal arrow indicates the crack-growth direction.

are quite similar to those seen on failure surfaces of tensile specimens [9–11]. Under cyclic loading, small step-like (slip or microcleavage) features are observed on platelet surfaces at high magnifications (Fig. 7(d) vs. Fig. 8(d)) which are quite different from features seen during monotonic fracture.

Fatigue crack paths in the lamellar microstructure are relatively linear compared with their monotonic counterparts [10,11], although they are more tortuous and deflected when compared with morphologies in the duplex microstructure (Fig. 6). During quasi-static fracture, cracks are found to arrest at laminate colonies oriented normal to the crack growth direction and/or deflect along the microlaminar interface, similar to reports in other lamellar γ-TiAl alloys [9–12]. In addition, microcracks nucleate ahead of the crack tip along the γ–α_2 or γ–γ interfaces and across lamellae, above and below the principal crack plane, resulting in uncracked ligament bridging by lamellar colonies. Such cracking processes are prevalent over length scales of about 2–3 mm under monotonic loading and enhance the fracture resistance of the lamellar γ-TiAl alloy. By contrast, crack deflection and microcracking effects under cyclic loading were limited to about 200–300 μm behind the crack tip (Fig. 6(b)).

4. Discussion

From the above results it can be inferred that cyclic loading is an important damage mechanism for subcritical crack growth in γ-TiAl based intermetallic alloys. The duplex microstructure of the Ti–47.3Al–2.3Nb–1.5Cr–0.4V alloy exhibits lower damage tolerance characterized by low toughness and an extreme sensitivity of cyclic crack-growth rates to the applied ΔK level. In contrast, the fully-lamellar structure displays improved damage tolerance at room temperature, despite potential limitations on tensile ductility and strength. Significant stable crack extension is observed following crack initiation at about 20 MPa $m^{1/2}$ with plateau toughness values from 30 to 40 MPa $m^{1/2}$ during fracture; the threshold for cyclic fatigue-crack propagation is about 10 MPa $m^{1/2}$.

Such microstructural differences in the crack-growth behavior of the γ-TiAl alloy may be correlated to

fractographic features noted during monotonic and cyclic loading. These observations suggest that the micromechanisms governing cyclic crack growth in γ-TiAl alloy are both intrinsic and extrinsic in nature. Crack-growth mechanisms under monotonic and cyclic loading are quite distinct. This is apparent in both microstructures from the fine, parallel slip-, microtwin-and/or microcleavage-like markings observed during cyclic fatigue, compared with the mostly transgranular cleavage failures seen during quasi-static fracture. As in metallic materials, the intrinsic fatigue-crack growth mechanism may be associated with the accumulation of irreversible strain at the crack tip through dislocation substructure development, alternative blunting and resharpening of the crack or deformation twinning [26].

In the duplex microstructure, intrinsic damage occurs in concert with quasi-static, fast fracture (cleavage) modes that are prevalent under cyclic loading conditions. Cyclic crack propagation is observed in a very narrow range of ΔK levels between 6 and 7 MPa $m^{1/2}$ ($K_{max} \sim 7$–8 MPa $m^{1/2}$) very close to the K_{Ic}, suggesting limited crack-tip plasticity despite higher tensile ductility of the duplex alloy. This factor, combined with lack of any significant crack-tip shielding, contributes to the lower fracture-crack growth resistance of the duplex microstructure.

Conversely, extrinsic crack-tip shielding effects are prominent and account for the superior fatigue and fracture properties of the lamellar alloy, although they are considerably more effective during monotonic fracture than under cyclic fatigue. Contributions to the fatigue-crack growth resistance of the lamellar structure are provided by crack deflection, microcracking ahead of the crack tip and resultant shear-ligament bridging by $\gamma + \alpha_2$ laminate colonies. However, the inherently small crack-opening displacements under cyclic loading restrict the extent of the bridging zones to within about 300 μm behind the crack tip, compared to a few millimeters under monotonic loading. In fact, at near-threshold stress intensities, back-face strain compliances estimates of the bridged crack length were approximately equal to the actual crack length, indicating minimal shielding; bridging effects, however, do become somewhat more prominent at higher ΔK levels. Thus, analogous to behavior in TiNb-reinforced TiAl composites [16,17], cyclic loading limits limits the role of crack-tip shielding, in this case primarily from shear-ligament bridging by lamellar colonies, in promoting resistance to crack growth.

In addition to crack deflection and bridging considerations, the improved fatigue-crack growth and fracture properties of the lamellar microstructure observed in the present study may also be associated with the large grain (or colony) size; this results in a lack of constraint in small laboratory test specimens as used in this study. With a grain size of about 1–2 mm and a sample thickness of 5 mm, the crack-growth rate response is averaged over approximately three grains through the thickness. Thus it cannot truly represent crack extension under true polycrystalline constraint, as experienced by the duplex microstructure. Previous studies on conventional ($\alpha + \beta$) titanium alloys [27–29] have shown that such constraint, assessed in terms of the ratio of sample thickness to colony size, influences the fatigue-crack growth resistance of different microstructures. Fatigue-crack propagation behavior of the lamellar alloy using large samples could not be evaluated in this study due to limitations on available material. The issue, however, is critical for the development and potential application of these dual-phase alloys and for understanding the micromechanisms influencing fatigue and fracture properties of γ-TiAl alloys in general.

5. Conclusions

From an experimental study on the ambient temperature fatigue-crack growth and fracture-toughness behavior of a two-phase ($\alpha_2 + \gamma$) Ti–47.3Al–2.3Nb–1.5Cr–0.4V alloy, processed in a fine duplex and a coarse lamellar microstructure, the following conclusions may be made.

(1) The lamellar microstructure exhibits superior fatigue-crack propagation and fracture resistance compared to the duplex microstructure. Measured fatigue thresholds in lamellar γ-TiAl under cyclic loading are about 10 MPa $m^{1/2}$, with a crack-initiation toughness of 20 MPa $m^{1/2}$ and stable crack growth up to a maximum of about 40 MPa $m^{1/2}$ under quasi-static loading; corresponding ΔK_{TH} and K_{IC} values for the duplex alloy are 6.5 and 10 MPa $m^{1/2}$, respectively. However, properties of the coarse lamellar microstructure may depend on laboratory test specimen size and geometry.

(2) The superior fatigue and fracture behavior of the lamellar microstructure is attributed to the role of extrinsic shielding from crack deflection, microcrack nucleation ahead of the crack tip and resultant shear-ligament bridging by intact lamellar colonies in the crack wake, akin to behavior in aligned composites. The influence of shielding and resultant toughening is considerably restricted under cyclic loading.

(3) Apart from extrinsic shielding considerations, fractographic evidence suggests that cyclic fatigue is associated with intrinsic damage and crack-

advance mechanisms distinct from those operating under monotonic loading. However, quasi-static fracture modes also play a prominent role during fatigue-crack growth in the γ-TiAl alloy, particularly at high ΔK levels.

Acknowledgments

This work was supported by the US Air Force Office of Scientific Research under Grant No. F49620-93-1-0107 (KTVR, CLM and ROR) with Dr. C.H. Ward as program manager and by the US Air Force Wright Laboratory, Materials Directorate under Contract No. F33615-91-C-5663 (Y.-W. Kim). Our thanks to Drs. C.H. Ward and Alan H. Rosenstein of the AFOSR for their continued support.

References

[1] Y-W. Kim, *J. Met., 41* (7) (1989) 24.
[2] Y-W. Kim, *Acta Metall., 40* (1992) 1121.
[3] M. Yamaguchi, *Mater. Sci. Technol., 8* (1992) 299.
[4] M. Yamaguchi and H. Inui, in R. Darolia, J.J. Lewandowski, C.T. Liu, P.L. Martin, D.B. Miracle and M.V. Nathal (eds.), *Structural Intermetallics*, TMS-AIME, Warrendale, PA, 1993, p. 127.
[5] S. Mitao, S. Tsuyama and K. Minikawa, *Mater. Sci. Eng., A143* (1991) 51.
[6] R. Gnanamoorthy, Y. Mutoh, N. Masahashi and M. Matsuo, *J. Mater. Sci., 28* (1993) 6631.
[7] H.E. Dève and A.G. Evans, *Acta Metall. Mater., 39* (1991) 1171.
[8] H.E. Dève, A.G. Evans and D.S. Shih, *Acta Metall. Mater., 40* (1992) 1259.
[9] Y-W. Kim and D.M. Dimiduk, *J. Met., 43* (8) (1991) 40.
[10] K.S. Chan and Y-W. Kim, *Metall. Trans. A, 23* (1992) 1663.
[11] K.S. Chan and Y-W. Kim, *Metall. Trans. A, 24* (1993) 113.
[12] K.S. Chan, *Metall. Trans. A, 24* (1993) 569.
[13] P.S. Pao, A. Pattnaik, S.J. Gill, D.J. Michel, C.R. Feng and C.R. Crowe, *Scripta Metall., 24* (1990) 1895.
[14] A.W. James and P. Bowen, *Mater. Sci. Eng., A153* (1992) 486.
[15] D.L. Davidson and J.B. Campbell, *Metall. Trans. A, 24* (1993) 1555.
[16] K.T. Venkateswara Rao, G.R. Odette and R.O. Ritchie, *Acta Metall. Mater., 40* (1992) 353.
[17] K.T. Venkateswara Rao, G.R. Odette and R.O. Ritchie, *Acta Metall. Mater., 42* (1994) 893.
[18] R.O. Ritchie and R.H. Dauskardt, *J. Ceram. Soc. Jpn., 99* (1991) 1047.
[19] R.H. Dauskardt, *Acta Metall. Mater., 41* (1993) 2765.
[20] K.S. Chan and Y-W. Kim, *Acta Metall. Mater., 42* (1994).
[21] *American Society for Testing and Materials Standard E647-91*, ASTM, 3.01 (1992) 674.
[22] R.O. Ritchie, W. Yu and R.J. Bucci, *Eng. Fract. Mech., 32* (1989) 361.
[23] *American Society for Testing and Materials Standard E399-90*, ASTM, 3.01 (1992) 506.
[24] R.O. Ritchie, *Int. Metall. Rev., 20* (1979) 205.
[25] K.T. Venkateswara Rao and R.O. Ritchie, *Int. Mater. Rev., 37* (1992) 153.
[26] S.M.L. Sastry and H.A. Lipsitt, *Metall. Trans. A, 8* (1977) 299.
[27] G.R. Yoder and D. Eylon, *Metall. Trans. A, 10* (1979) 1808.
[28] D. Eylon and P.J. Bania, *Metall. Trans. A, 9* (1978) 1273.
[29] G.R. Yoder, L.A. Cooley and T.W. Crooker, *Metall. Trans. A, 8* (1977) 1737.